

**THE STRUCTURAL MCHANICAL, VIBRATIONAL AND ELECTRONIC  
PROPERTIES OF KNbO<sub>3</sub> PEROVSKITE USING DENSITY FUNCTION THEORY**

**BY**

**EFE EMMANUEL**

**PSC2208257**

**DEPARTNIENT OF PHYSICS  
FACULTY OF PHYSICAL SCIENCES  
UNIVERSITY OF BENIN  
BENIN CITY**

**NOVENBER, 2025**

**THE STRUCTURAL MCHANICAL, VIBRATIONAL AND ELECTRONIC  
PROPERTIES OF KNbO<sub>3</sub> PEROVSKITE USING DENSITY FUNCTION THEORY**

**BY**

**EFE EMMANUEL**

**PSC2208257**

**DEPARTNIENT OF PHYSICS  
FACULTY OF PHYSICAL SCIENCES  
UNIVERSITY OF BENIN  
BENIN CITY**

**IN PARTIAL FULFILMENT OF THE REQUIREMENTS FOR THE AWARD OF  
BACHELOR OF SCIENCE (B.Sc.) IN INDUSTRIAL PHYSICS.**

**NOVENBER, 2025**

**CERTIFICATION**

THIS IS TO CERTIFY THAT THIS PROJECT WORK WAS CARRIED OUT BY EFE  
EMMAUEL WTH MATRICULATION NUMBER PSC2208257, OF THE DEPARTMENT  
OF PHYSICS FACULTY OF PHYSICAL SCIENCES UNIVERSITY OF BENIN, CITY,  
EDO STAT  
E NIGERIA

DR. M.I BABALOLA  
(Project Supervisor)

Date

PROF. C. O. AIGBOGUN  
(Head of Department)

Date

External Examiner

Date

### **DEDICATION**

This work is firstly dedicated to God, my lecturers mentors and friends whose advice and expertise have been invaluable to my academic career. My knowledge and development have been influenced by their tolerance and insight. My family has been my greatest source of strength because of their unwavering support, encouragement, and sacrifices, to whom I sincerely dedicate this endeavor Their faith in my potential has motivated me to pursue greatness.

**CERTIFICATE OF DISSERTATION ON PLAGIARISM**

### **ACKNOWLEDGEMENT**

I want to thank Dr. M.I Babalola my project supervisor, whose advice clarifications, tolerance, and encouragement were invaluable in helping me finish this study.

Additionally, I would like to thank Chukwu Emmanuel, Friday John Tobiloba who were my project mates for their cooperation and friendship throughout this endeavour.

### **ABSTRACT**

In my work the mechanical, structural, vibration, and electronic properties of  $\text{KNbO}_3$  perovskite using density functional theory (DFT). the aim of this research is to provide understanding of its characteristics and potential applications in ferroelectric devices.

In agreement with previously published theoretical values, Phonon dispersion analysis was conducted to assess the dynamical stability and vibrational behaviour of the crystal. In addition, the electronic band structure and density of states (DOS) were analyzed to understand the nature of its bonding and band gap.

This work gave explanation to the computational techniques used and offer a rigid understanding of the structural, mechanical, and electrical properties of  $\text{KNbO}_3$  perovskite.

## TABLE OF CONTENTS

COVER PAGE.....	i
TITLE PAGE.....	ii
CERTIFICATION.....	iii
DEDICATION.....	iv
CERTIFICATE OF DISSERTATION ON PLAGIARISM.....	v
ACKNOWLEDGEMENT.....	vi
ABSTRACT.....	vii
TABLE OF CONTENTS.....	viii
CHAPTER ONE.....	1
INTRODUCTION.....	1
1.1 Origin of Perovskite.....	1
1.2.1 Optical Properties.....	2
1.2.2 Multiferroicity.....	2
1.2.3 Piezoelectricity.....	3
1.2.4 Catalytic Activity.....	3
1.2.5 Superconductivity.....	3
1.3 Applications of Perovskites.....	3
1.3.1 Perovskite Solar Cells (PSCs).....	3
1.3.2 Perovskite Light-Emitting Diodes (PeLEDs).....	4
1.3.3 Perovskite Photodetectors.....	4
1.3.4 Perovskite Dielectrics and Ferroelectric Devices.....	4
1.3.5 Perovskite Catalysis and Fuel Cells.....	5
1.4 Aim and Objectives.....	5
CHAPTER TWO.....	6

LITERATURE REVIEW .....	6
2.1 Overview and DFT Methodology .....	6
2.1.2 structural properties .....	6
2.1.3. Mechanical (elastic) properties .....	7
2.1.4. vibrational (phonon) properties.....	7
2.1.5. electronic structure and optical properties .....	7
CHAPTER THREE .....	9
3.1. Methodology .....	9
3.1.1. Density Functional Theory (DFT) .....	9
3.1.3. Local Density Approximation (LDA).....	11
3.1.3.1 Khon Shan Equation .....	12
3.1.4.2. Quantum Espresso (QE) .....	15
3.1.4.3. Post Processing .....	20
3.1.4.4. Band Structure .....	21
3.1.4.5. Density of State (DOS) .....	22
3.1.5. Computational Details .....	22
3.1.5.1 Convergence Test (Optimization).....	22
3.1.5.2. Kinetic Energy cut-off (ecutwfc).....	22
3.1.6. POST PROCESSING .....	25
CHAPTER FOUR.....	26
4.1 Results and Discussion .....	26
4.1.1 Structural Properties.....	26
4.1.2 Mechanical Properties.....	26
4.1.3 Electronic and Magnetic Properties .....	29
4.1.4 Phonon and Vibrational Properties .....	31

4.1.4.1 Overview of Phonon and Vibrational Properties .....	31
4.1.4.2 Phonon Dispersion Relation .....	31
4.1.4.3 Vibrational Modes and Their Origin.....	32
4.1.4.4 Phonon Density of States (PhDOS) .....	32
4.1.4.5 Ferroelectric and Lattice-Dynamical Implications .....	33
4.1.4.6 Thermal and Elastic Insights.....	33
CHAPTER FIVE .....	36
5.1 Findings and Conclusion.....	36
5.2 Suggestions for Further Studies .....	36
REFERENCES .....	37

## CHAPTER ONE

### INTRODUCTION

#### 1.1 Origin of Perovskite

The term "perovskite" refers to any compound with the general formula  $(AB)X_3$ , characterized by a crystal structure similar to that of the mineral perovskite, which consists of calcium titanium oxide ( $\text{CaTiO}_3$ ). This mineral was named after the Russian mineralogist L.

A. Perovskite (1792—1856) and was first discovered in the Ural Mountains of Russia in 1839.

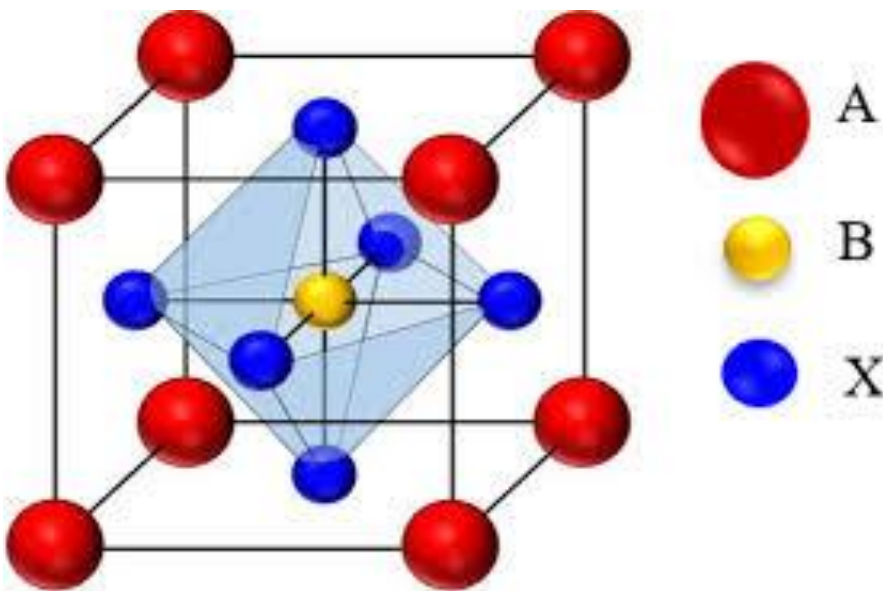


Fig 1.1: An ideal Perovskite structure

The following are properties of Perovskite:

The A-site, typically occupied by larger cations, can host elements from Groups 1, 2, or the lanthanide series, fitting into the 12-coordinate cavities formed by the BXs network.

The B-site, found at the octahedral centers, is usually occupied by smaller cations, often transition metals (Groups 3—12) or main group elements like tin.

The X-site is commonly filled by oxygen (O<sup>2-</sup>) but can also include heavier halide ions such as Cl<sup>-</sup> or Br<sup>-</sup>.

### **Properties of Perovskite**

Since perovskite materials have a unique chemical structure and stoichiometry, they have a wide range of properties, some of which are listed here:

#### **1.2.1 Optical Properties**

Perovskite crystals such as BaTiO<sub>3</sub> and SrTiO<sub>3</sub> possess stable refractive indices across temperature ranges and transmit light in the infrared spectrum. Materials like KTN display strong electro-optic responses, making them useful in laser and optical communication systems. Additionally, rare-earth-doped perovskite oxides and environmentally friendly compounds like BaZrO<sub>3</sub> exhibit visible photoluminescence, with potential applications in lighting, displays, and scintillators (Kim *et al.*, 2005).

#### **1.2.2 Multiferroicity**

Multiferroic materials exhibit multiple ferroic properties—such as ferroelectricity, ferromagnetism, and ferroelasticity simultaneously. Many perovskite-type oxides, including ferrites and rare-earth manganites, demonstrate multiferroicity at room temperature. For instance, bismuth ferrite (BiFeO<sub>3</sub>) displays both ferroelectric and antiferromagnetic order well above ambient temperature (Singh *et al.*, 2011). These materials are highly promising for spintronic and multifunctional device applications.

### **1.2.3 Piezoelectricity**

Perovskite-based ceramics of the form  $A_2B_4O_{12}$  exhibit piezoelectricity, where mechanical stress generates an electric charge and vice versa (Aksel *et al.*, 2011). This bidirectional property enables applications in sensors, actuators, and transducers.

### **1.2.4 Catalytic Activity**

Perovskites possess excellent catalytic activity and chemical stability, allowing them to facilitate redox and oxidation reactions. They are categorized as oxidation or oxygen-activated catalysts, making them valuable for environmental remediation and energy conversion processes (Roni, 2018).

### **1.2.5 Superconductivity**

Certain copper-containing perovskites demonstrate high-temperature superconductivity, where electrical resistance drops to zero below a critical temperature. The La—Ba—Cu—O perovskite system was among the first discovered examples. These oxides have since become a major class of high- $T_p$  superconductors, surpassing earlier intermetallic systems (Cava, 2008).

## **1.3 Applications of Perovskites**

Thanks to their exceptional physical properties and compositional versatility, perovskite materials are used in a variety of advanced technologies, including solar cells, light-emitting diodes, photodetectors, ferroelectric devices, and fuel cells.

### **1.3.1 Perovskite Solar Cells (PSCs)**

Perovskite solar cells employ materials such as  $\text{MAPbI}_3$  as light absorbers, efficiently converting sunlight into electrical energy.

**Advantages:**

- I High power conversion efficiency (>25%)
- II Low-cost, solution-based fabrication
- III Lightweight and flexible structure
- IV Tunable bandgap for tandem configurations with silicon

**1.3.2 Perovskite Light-Emitting Diodes (PeLEDs)**

In PeLEDs, electrons and holes recombine within the perovskite emissive layer to generate light.

**Advantages:**

- I High luminescence efficiency comparable to OLEDs and QLEDs
- II Tunable emission across I-IV—NIR ranges
- III High color purity with narrow bandwidth

**1.3.3 Perovskite Photodetectors**

Perovskite-based photodetectors convert incident light into electrical signals with high efficiency.

**Advantages:**

- I Broad spectral response (UV—NIR)
- II High sensitivity and responsivity
- III Cost-effective, large-area fabrication via solution processing

**1.3.4 Perovskite Dielectrics and Ferroelectric Devices**

Ferroelectric perovskites such as BaTiO<sub>3</sub> and PbTiO<sub>3</sub> exhibit large dielectric constants and switchable polarization.

**Applications:**

- I Capacitors with high energy storage
- II Non-volatile FeRAM memory
- III Tunable microwave component

**1.3.5 Perovskite Catalysis and Fuel Cells**

Perovskites like  $\text{La Sr . MnO}_3$  and  $\text{LaFeO}_3$  serve as electrodes in solid oxide fuel cells (SOFCs) and as catalysts for oxygen reduction and evolution reactions (ORR/OER).

**Advantages:**

- I Excellent oxygen-ion conductivity
- II Cost-effective alternative to noble metals
- III High-temperature stability for long-term operation

**1.4 Aim and Objectives****Aim:**

To investigate the ground-state energy and physical properties of  $\text{RbNbO}_3$  perovskite using Density Functional Theory.

**Objectives:**

1 To calculate the structural properties (lattice constant, bulk modulus, and pressure derivatives).

To determine the electronic properties (band structure, density of states, and material type).

To evaluate the mechanical properties (elastic constants, shear modulus, Young's modulus, etc.).

Commented [j1]:

## CHAPTER TWO

### LITERATURE REVIEW

#### 2.1 Overview and DFT Methodology

Density functional theory (DFT) has been widely used to study KNBO<sub>3</sub> in its multiple polymorphs (cubic, tetragonal, orthorhombic, rhombohedral). Researchers typically employ local/semilocal functionals (lda, pbe/pbesol) for structural and elastic properties and hybrid functionals (hse06) or many body corrections for more reliable band-gap predictions. common computational approaches include plane-wave p w or pseudopotential methods and all electron flapw/lmto for higher-accuracy electronic/phonon work.

these methodological choices strongly affect predicted lattice parameters, phonon frequencies and band gaps, so cross-study comparisons should account for the chosen functional and pseudopotential.

#### 2.1.2 structural properties

Multiple dft studies report equilibrium lattice parameters and relative stability of knb03 phases. wan *et al*

l. (2012) performed an extensive first-principles study across the experimentally known phases and reported dft optimized lattice constants and internal coordinates for tetragonal, orthorhombic and rhombohedral phases, showing good agreement with experiment when using appropriate functionals and convergence settings. lu (2015) and xu *et al.* (2020) similarly provided cubic(001) and pressure-dependant structural data and highlighted volume/phasetrans under strain/pressure. overall, semilocal gga (pbe /pbesol) tends to slightly overestimate volumes compared to experiment, while Ida undgestimates the m; pbesol often gives improved lattice constants for perovskite oxides.

### **2.1.3. Mechanical (elastic) properties**

Elastic constants and derived moduli (bulk shear, young modulus, poisson ratio) for knb03 have been calculated from stress—strain relationships in several dft works. wan *et al.* (2012) computed the full elastic tensors for the known phases and assessed mechanical stability criteria; experimental brillouin-scattering elastic constants for orthorhombic knb03 provide benchmarks for dft results. pressure-dependant elastic behavior has also been explored (xu *et al.*, 2020), showing stiffening with compression and indicating mechanically stable perovskite phases across a range of pressures. these studies are useful when comparing your calculated bulk modulus and elastic constants.

### **2.1.4. vibrational (phonon) properties**

Phonon calculations are central to assessing dynamical stability and ferroelectric soft modes in knb03. early frozen-phonon/linear-response studies (postnikov *et al.*, 1994) computed y-point transverse-optical phonons and identified modes related to ferroelectricity. more recent work emphasizes anharmonicity and temperature dependence: self-consistent phonon (SCP) and anharmonic force constant methods show substantial anharmonic renormalization of soft modes and improve agreement with finite-T experiments (kim *et al.*, 2023). These studies highlight that harmonic phonons alone can mischaracterize soft mode frequencies and phase transition behavior in ferroelectric perovskites.

### **2.1.5. electronic structure and optical properties**

Dft band-structure and dos studies find knb03 to be a widegap oxide semiconductor whose gap and band-edge character depend on phase and computational method. semilocal dft (pbe) typically underestimates the gap (report.0—2.0 eV depending on phase and parameter choices), while hybrid functionals (hse06) and gw corrections give larger, experimentally more realistic values liang *et al.* (2019) used hse06 to refine band-gap predictions and to study transition-metal substitution effects on band edges. spectroscopy-focused dft work

(e.g., electron-energy-loss / dielectric function simulations) connects band-structure features with optical spectra and plasmons. pressure studies (yaseen *et al.*, 2021) indicate gap changes and even indirect and direct transitions under very large compression.

## CHAPTER THREE

### 3.1. Methodology

#### 3.1.1. Density Functional Theory (DFT)

One of the most popular and effective quantum mechanical theories for describing matter in physics and chemistry is density functional theory (DFT), which is used to determine among other things the band structure of materials and the binding energy of molecules. DFT has been used to investigate a variety of phenomena, such as relativistic effects in heavy elements and atomic nuclei superconductivity, atoms under intense laser pulses, classical liquids, and magnetic properties of alloys.

In quantum mechanics, the wave function of a system contains all the possible information about the system, which depends on the electronic coordinates; the wave function is computed without taking relativity into account using the Schrodinger equation which computes the wave function of a single electron moving with a potential. This fact accounts for the versatility of DFT which is based on the universality of its fundamental concepts and the flexibility with which they can be applied.

Ab initio, without the need for higher-order factors like basic material properties, DFT calculations in computational material science allow the computation and prediction of material behavior based on quantum mechanical principles. Current DFT techniques assess the electronic structure of a system by using a potential acting on its electrons. The effective potential,  $V_{\text{eff}}$ , which denotes inter-electronic interactions, and the external potentials,  $V_{\text{ext}}$ , which are determined only by the structure and elemental makeup of the system, add up to the total potential,  $V$ .

DFT provides a more flexible solution to the many-body problem by studying a set of non-interacting electron Schrodinger equations, also known as Kohn-Sham equations, for a representative supercell of a material with  $n$  electrons. The electron density,  $n(\mathbf{r})$ , is the key

variable in DFT and is determined by the square of the wave function for a normalized wave function.

$$n(\mathbf{r}) = N \int d^3r_2 \dots \int d^3r_N \psi^*(\mathbf{r}_1, \mathbf{r}_2, \dots, \mathbf{r}_N) \psi(\mathbf{r}_1, \mathbf{r}_2, \dots, \mathbf{r}_N) \dots \dots \dots (3.1)$$

After decades of struggle, several successful methods have been developed to solve Schrodinger's equation, such as diagrammatic perturbation theory in physics, which is based on Feynman diagrams and Green's functions, and configuration interaction (CI) methods in chemistry, which involve systematic expansion in Slater determinants. Although there are many specialized methods available, these methods are computationally intensive and may not be feasible for large, complex systems. DFT provides a suitable alternative, which may be less precise but is more flexible. The density-functional approach can be summed up as follows:

$$n(\mathbf{r}) = (r_1, \dots, r_N) = V(\mathbf{r}) \dots \dots \dots (3.2)$$

### 3.1.2 Generalized Gradient Approximation (GGA)

In ab initio total energy calculations for exchange-correlation energy in density-functional theory, the generalized gradient approximation, or GGAJ is currently gaining popularity as a less complicated substitute for the local density approximation (LDA) (Jones *et al.*, 1898). In atomic and molecular physics, where experimental data is more easily accessible and LDA overestimates by 20% or more, it is not as accurate as it is in condensed matter systems.

Gradient corrections are introduced to address the issue of underestimation of bond lengths caused by cohesive energies and bond strength in molecules and solids. By writing the exchange-correlation functional as a function of both the local density and the local gradient of the density, the non-homogeneity of the electron density can be accounted for. This represents a logical step beyond LDA, which only considers the density at a given point.

### 3.1.3. Local Density Approximation (LDA)

The exchange-correlation (XC) energy functional in density functional theory (DFT) is estimated using the local density approximation (LDA), a collection of approximations that only use the electronic density information from the Kohn-Sham orbitals. Local approximations of the XC energy can be produced using a variety of methods; the homogeneous electron gas (HEG) model offers many useful local approximations. Functionals based on the HEG approximation are frequently used interchangeably with LDA when applied to real systems, such as molecules and solids. A local-density approximation for the XC energy in unpolarized systems is commonly written as follows:

$$E_{XC}^{LDA}[P] = \int d\mathbf{r} \, n(\mathbf{r}) \epsilon_{XC}(n(\mathbf{r})) \quad (3.3)$$

The electronic density  $n$  and the exchange-correlation energy per particle of a homogeneous electron plasma with charge density  $p$  are used to describe the exchange-correlation energy  $E_{XC}$  per particle, which is linearly divided into exchange and correlation components.

$$E_{XC} = E_X + E_C \quad (3.4)$$

The exchange term assumes a simple analytical form of HEG. Solid state physicists commonly employ GGAs in ab-initio DFT studies to interpret electronic and magnetic interactions in semiconductor materials, such as semiconductor oxides and spintronics, but the precise correlation density limiting expressions are the only ones known, leading to a variety of approximations for  $E_C$ . The significance of these computational studies comes from the complexity of the system, which makes it extremely sensitive to synthesis parameters and requires first-principles based analysis. LDA in conjunction with simulated packages is frequently used to estimate the Fermi level and structure in perovskites. On the other hand, an underestimating of band gap values, which is frequently linked to LDA and GGA approximations, can result in inaccurate estimates of impurity effects, conductivity influenced by carriers, and magnetism mediated by carriers in these systems. Since 1998, the Rayleigh

theorem for eigenvalues has been applied using LDA potentials, yielding generally accurate band gap predictions for materials. The context of the two DFT theorems' assertions in the study of density functional theory clarifies a widespread misunderstanding about the second DFT theorem.

### 3.1.3.1 Kohn-Shan Equation

For a hypothetical system of non-interacting particles, usually electrons, the Kohn-Shan equation is a one-electron Schrödinger equation that produces the same electron density as a specific system of interacting particles. A local effective potential, commonly represented as  $V(r)$  or  $V_{\text{eff}}(r)$ , defines this equation by functioning as a false external potential on the non-interacting particles. A set of orbitals that are the lowest-energy solutions to the Kohn-Shan equation are used to generate the single Slater determinant that is the Kohn-Shan wave function. (Walter Kohn and Lu Jeu Shan 1965)

$$\left(-\frac{\hbar^2}{2m}\nabla^2 + V_{\text{eff}}(r)\right)\varphi_i = \epsilon_i \varphi_i \dots \dots \dots (3.5)$$

One common way to represent the Kohn-Shan equation is as an eigenvalue equation itself. The density for an N-particle system is determined by the sum of the squares of the absolute values of the Kohn-Shan orbitals, and this equation includes the orbital energy ( $\epsilon_i$ ) of the corresponding Kohn-Shan orbital.

$$P(r) = \sum_1^N |\varphi_i(r)|^2 \dots \dots \dots (3.6)$$

### 3.1.4. Pseudopotentials and Applications

This chapter examines both ab-initio and empirical pseudopotentials, as well as their various applications. The concept of the pseudopotential, also referred to as the standard model for condensed phases, has greatly advanced our understanding of semiconductor electrical structure. The first applications of empirical pseudopotentials were to describe the optical and dielectric properties of tetrahedral semiconductors, and it was later demonstrated that the

resulting image of a one-electron band structure was valid. These band structures were developed more than 30 years ago, but they are still largely accurate. Current concepts for understanding the chemical bond in solids rely on the combination of density functional theory and pseudopotentials, which have been used to accurately predict the compressibility, vibration modes, phase stability, and structural properties of semiconductors in multiple states.

The intrinsic energy and spatial separation of valence and core electrons provide the basis of the pseudopotential idea. Gaussian type functions are commonly used to fit pseudo potentials in traditional quantum espresso computing systems. Within the framework of density functional theory (DFT), pseudopotentials can be created in a number of ways, such as by employing parameterized analytical pseudopotentials or by constructing pseudo potentials using pseudo-orbitals obtained from atomic calculations. Since the matrix elements of an effective Hamiltonian can be computed directly using either analytical or numerical basis sets (or a mixed one), the discrete variation method (DVM), a specific implementation of numerical integration for solving the DFT one electron equations, does not require the fitting of pseudoorbitals to any analytical functions.

The simplicity of controlling the precision of a plane wave basis is one of its benefits, but a major disadvantage is that the size of the basis set needed for a particular system is frequently far greater than what would be required with a localized basis set. This is due to the fact that orbitals in condensed matter systems have a tendency to oscillate more quickly near atomic nuclei and more gradually in other areas. Since most of the space in the cells does not include rapidly oscillating orbitals, a high cut-off energy is required to include plane waves with short wavelengths in order to represent this rapid oscillation. However, the majority of the processing expenses related to these plane waves are wasted. This issue can be considerably lessened by using pseudopotential in combination with plane waves.

Pseudopotential allows for more effective computations of the electronic structure of the system by substituting a smoother easier-to-manage potential that has the same effect on the valence electrons as the genuine potential for the fast-oscillating core electrons. We take note of the following information regarding orbitals in the condensed matter system in order to comprehend what pseudopotentials are:

1. Electrons that are firmly attached to an atom's nucleus and inhabit lower energy orbitals are known as core electrons. They have a high degree of localization around the nucleus and are typically unaffected by the atom's chemical surroundings.

2. Because they must be orthogonal to the core electrons, many of the fast oscillations in the orbitals of non-core electrons close to atomic nuclei can be ignored. This implies that the orbitals of the non-core electrons must be built differently from those of the core electrons, which will suppress some oscillations.

The nuclear charge is effectively represented by pseudopotential theory, which substitutes a false potential for the core electrons and guarantees that the behavior of the valence electrons stays constant after a specific distance from the nucleus. As long as the radius does not overlap with areas engaged in chemical bonding, the pseudopotential approximation should not substantially change the behavior of condensed matter, which is determined by interatomic interactions. There are four ways that employing pseudopotential lowers the computing cost of computations:

The number of Kohn-Shan orbitals is reduced by removing core electrons from the calculations, which also reduces the amount of memory required to store the orbitals and the amount of time required to orthogonalize a collection of orbitals.

The corresponding orbitals close to the nucleus oscillate less when there are no core electrons for the valence electrons to be orthogonal to. This makes it possible to represent orbitals with a lower cut-off energy, which speeds up calculations and uses less memory. Efficiency can be

greatly increased by lowering the cut-off energy, which frequently leads to orders of magnitude gains in computational performance.

Because the pseudopotential's form is modifiable rather than fixed for a particular element, optimization to obtain the lowest cut-off energy is possible. This enhancement increases calculation efficiency by reducing memory usage and speeding up processing.

Because the pseudopotential's form is modifiable rather than fixed for a particular element, optimization to obtain the lowest cut-off energy is possible. This enhancement increases calculation efficiency by reducing memory usage and speeding up processing.

#### 3.1.4.1. Ultra Soft Pseudopotentials (USPP)

Ultrasoft pseudopotentials relax the norm-conserving criterion to further reduce the required size of the basis set, however this results in a generalized eigenvalue problem. David Vanderbilt, April 1990

#### 3.1.4.2. Quantum Espresso (QE)

Released under the GNU General Public License, Quantum ESPRESSO is a publicly available package of quantum chemistry methods for electronic structure computations and materials modelling. It is based on norm-conserving and ultrasoft pseudopotentials, plane wave basis sets, and Density Functional Theory. The CNR-IOM DEMOCRITOS National Simulation Centre in Trieste, Italy, is the leader of the open-source package, called ESPRESSO in partnership with other international research institutions like MIT, Princeton University, the University of Minnesota, and the Ecole Polytechnique Federal de Lausanne. (Giannozzi Paolo, and others, 2009). Essential plane wave DFT procedures are provided by the package's core programs, which are primarily written in Fortran-90 with some parts in C or Fortran 77. These key programs include pwsef, which solves the self-consistent Kohn and Sham equations in a periodic solid, Post Proc, which analyse and charts data, and CR which

deals with Car-Parrinello molecular dynamics. Other packages include Atomic for generating pseudopotentials,

NEB for calculating reaction routes and energy barriers, and Phonon for computing second and third order derivatives of the energy with regard to atomic displacement using Density Functional Perturbation Theory.

The foundation of Quantum ESPRESSO is the Plane Wave-Self-Consistent Field (PWSCF) component of the Open-Source Package for Research in Electronic Structure, Simulation, and Optimization or ESPRESSO which was first made available on June 15 2001, and has since been continuously developed and improved by the international consortium of research centres and organizations that oversee the project.

The following shell scripts were used for optimization of parameters;

#### **Create 1 sh**

```
#!/bin/sh

sys='knbo3'

for CUTOFF in 30 35 40 45 50 55 60 65 70 75 80
do

cat > $sys.scf.in << EOF
&CONTROL
  calculation = 'scf'
  prefix = 'kNbO3',
  outdir = './',
  pseudo_dir = '/home/wintech/PSEUDOPOTENTIALS/',
/
&SYSTEM
 ibrav=1,
  celldm(1) = 7.928,
  nat = 5,
  ntyp = 3,
  ecutwfc = $CUTOFF,
  occupations = 'smearing',
  smearing = 'mp',
  degauss = 0.02,
```

```

/
&ELECTRONS
  conv_thr = 1.0d-8,
  mixing_beta = 0.7,
  diagonalization = 'david',
/
ATOMIC_SPECIES
K 39.0983 K.pbe-spn-kjpaw_psl.1.0.0.UPF
Nb 92.9064 Nb.pbe-spn-kjpaw_psl.0.3.0.UPF
O 15.9994 O.pbe-n-kjpaw_psl.1.0.0.UPF

ATOMIC_POSITIONS {crystal}
K 0.0 0.0 0.0
Nb 0.5 0.5 0.5
O 0.5 0.0 0.5
O 0.0 0.5 0.5
O 0.5 0.5 0.0

K_POINTS {automatic}
6 6 6 0 0 0

EOF

mpirun --use-hwthread-cpus -np 4 ~/qe-6.7/bin/pw.x < $sys.scf.in > $sys.scf.out
awk '/kinetic/{alat=$(NF-1)}!/{print alat, $(NF-1)}' $sys.scf.out >> ecut

done

Create 2 sh

#!/bin/sh

sys='knbo3'

for alat in 3 4 5 6 7 8 9 10 11
do

# self-consistent calculation
cat > $sys.scf.$alat.in << EOF
&CONTROL
  calculation = 'scf'
  prefix = 'kNbO3',
  outdir = './',
  pseudo_dir = '/home/wintech/PSEUDOPOTENTIALS/',
/
&SYSTEM
 ibrav = 1,
  celldm(1) = 7.928,
  nat = 5,

```

```

ntyp = 3,
ecutwfc = 75,
occupations = 'smearing',
smearing = 'mp',
degauss = 0.02,
nspin = 1,
/
&ELECTRONS
conv_thr = 1.0d-8,
mixing_beta = 0.7,
diagonalization = 'david',
/
ATOMIC_SPECIES
K 39.0983 K.pbe-spn-kjpaw_psl.1.0.0.UPF
Nb 92.9064 Nb.pbe-spn-kjpaw_psl.0.3.0.UPF
O 15.9994 O.pbe-n-kjpaw_psl.1.0.0.UPF

ATOMIC_POSITIONS {crystal}
K 0.0 0.0 0.0
Nb 0.5 0.5 0.5
O 0.5 0.0 0.5
O 0.0 0.5 0.5
O 0.5 0.5 0.0

K_POINTS {automatic}
$alat $alat $alat 0 0 0

EOF

mpirun --use-hwthread-cpus -np 4 ~/qe-6.7/bin/pw.x < $sys.scf.$alat.in > $sys.scf.$alat.out

done

Create 3 sh

#!/bin/bash
for LA in -0.5 -0.4 -0.3 -0.2 -0.1 0.0 0.1 0.2 0.3 0.4 0.5 ;
#for LAT in 2 4 6 8 10 12 14 16;
do
LAT=`echo $LA | awk '{print($1+7.928)}'`

sys=knbo3

cat> $sys.scf.in << EOF
&CONTROL
calculation = 'scf'
prefix = 'KNbO3',

```

```

outdir = './',
pseudo_dir = '/home/wintech/PSEUDOPOTENTIALS',

/
&SYSTEM
ibrav = 1,
celldm(1) = $LAT,
nat = 5,
ntyp = 3,
ecutwfc = 75,
occupations = 'smearing',
smearing = 'mp',
degauss = 0.02,
nspin = 1,
/
&ELECTRONS
conv_thr = 1.0d-8,
mixing_beta = 0.7,
diagonalization = 'david',
/
ATOMIC_SPECIES
K 39.0983 K.pbe-spn-kjpaw_psl.1.0.0.UPF
Nb 92.9064 Nb.pbe-spn-kjpaw_psl.0.3.0.UPF
O 15.9994 O.pbe-n-kjpaw_psl.1.0.0.UPF

ATOMIC_POSITIONS {crystal}
K 0.0 0.0 0.0
Nb 0.5 0.5 0.5
O 0.5 0.0 0.5
O 0.0 0.5 0.5
O 0.5 0.5 0.0

K_POINTS {automatic}
6 6 6 0 0 0
EOF

mpirun --oversubscribe -np 4 ~/qe-6.7/bin/pw.x < $sys.scf.in > $sys.scf.out

awk '/lattice/{alat=$(NF-1)}!/{print alat, $(NF-1)}' $sys.scf.out >> alat

done
#ev.x calculation
~/qe-6.7/bin/ev.x

```

### 3.1.4.3. Post Processing

The software for post-processing computations was originally built by Stefano Baroni, Stefano de Gironcoli, Andrea Dal Corso (from SISSA), and Paolo Giannozzi (from the University of Udine), together with several other authors. ([www. quantum-espresso-org](http://www.quantum-espresso.org)) Plotting bands and computing the density of states (DOS) are two further small calculations we perform after finishing the self-consistent calculation. The following are the main post-processing programs that carry out further computations and retrieve the required data/files from the PW

SCF calculations:

1. pw.x: We use this command to run input files of scf and nscf calculations of energy and wave functions at each and every point. It produces output files for the energy calculation at every k-point.
2. bands.x: In order to prepare the data for processing, this pulls the files from the PWSCF computations and logs the eigenvalues at various k-points along with the associated energy values. The symmetry analysis of the band structure is likewise carried out using the codes bands.x.
3. plotband.x: Auxiliary codes plotbandx read the output files from bands.x directly and transform them to a plottable format. The values of the k-points must be placed in the proper order; otherwise, if the k-points are not arranged along lines or if two consecutive points are the same, surprising plots may emerge. As a result, selecting the k-point sequence correctly is crucial.
4. dos.x: It helps to calculate the electronic density of states at different k-points.
- 5 thermo\_pw.x: It is a Fortran driver that leverages Quantum ESPRESSO (QE) routines as the underlying engine for the parallel and/or automatic computation of material properties. It

generates postscript figures of some material properties after reading the same input as the QE PW.x code. (github.io)

#### **3.1.4.4. Band Structure**

As the basis of most crystal properties, the band structure of a solid can be used to determine various electrical properties. The electronic band structure is a commonly used analytical technique in the first principles electronic structure calculation of crystals, especially within the Kohn-Sham framework of density functional theory. It provides the electronic levels in (perfect) crystal formations, which are identified by a band index ( $n$ ) and a Bloch vector ( $K$ ), an element of reciprocal space, measured in length units, and typically limited to the first Brillouin Zone. (Andreas Wacker, 2010). The close packing of atoms in a solid causes their interaction to disturb the initial atomic levels when a large number of atoms are brought together. Since no two electrons can occupy the same energy state, all of the electrons in the orbitals are filled up according to Pauli's Exclusion Principle.

The electrons in the inner shell of a band are least affected by interatomic interactions, whereas the electrons in the valence band, which are nearest to adjacent ions, are most affected. This leads to the establishment of an energy continuum in which separate levels created by individual atoms cannot be recognized. A single, sharp level splits when two atoms are close to one another.

A solid's band structure can be utilized to identify its different electrical and optical properties. According to band theory, the measurement of the band gap identifies the type of solid. The pseudopotential and plane wave basis set approaches are used in density functional theory (DFT) to calculate the band structures. The Generalized Gradient Approximation (GGA) is used to treat the exchange correlation functional as the Perdew-Burke-Ernzerhof (PBE) functional.

#### **3.1.4.5. Density of State (DOS)**

The number of states that particles within a specific energy range can occupy per unit energy is known as the "Density of States" (DOS) (Walter, 1989). It is defined as the number of quantum states per unit of energy range and, in other words, is a measure of the concentration of quantum states in a system. In solid state and condensed matter physics, the density of states is important because it may be used to calculate a number of parameters that provide information about a wide range of electronic, magnetic, and transport properties.

#### **3.1.5. Computational Details**

##### **3.1.5.1 Convergence Test (Optimization)**

The self-consistent field (SCF) calculations were performed to ascertain fundamental parameters, specifically:

1. The kinetic energy cut-off for the k-points grid and plane wave basis.
2. The lattice parameters, which were obtained through energy minimization.

These parameters were evaluated by examining the convergence of the total energy with respect to each of these parameters individually.

##### **3.1.5.2. Kinetic Energy cut-off (ecutwfc)**

The kinetic energy cut-off, `ecutwfc`, measured in Ry determines the dimension of the plane-wave (PW) basis sets used to expand the wave function (Kohn-Sham orbitals). The closeness of the interactions determines the size of the kinetic energy cut-off in a periodic system. A more accurate result can be obtained by include long-range interactions by raising the cut-off energy. Nevertheless doing so necessitates using greater processing power. A modest energy cut-off could lead to inaccurate results even though the computations are reasonably priced. Determining the ideal cut-off energy value is so crucial.

### **CELL DIMENSION (LATTICE PARAMETER)**

The orderly arrangement of atoms in three dimensions, or the crystal lattice, is described by the lattice constant, whether or not it is an atomic attribute. It is normally measured in angstroms (Å), and for most crystals, its value is a few angstroms. The length of the lattice's repeat unit is essentially represented by the lattice constant.

### **K-POINTS GRID**

A dense enough grid of k-points is needed to capture periodicity, and a large number of grid points is essential for discretely representing interactions in the Brillouin zone, but because of practical computational resource constraints, the number of k-points must often be optimized using a rectangular grid of points with dimensions  $k \times k \times k$ , evenly distributed throughout the Brillouin zone, called the kpoints grid.

### **BAND STRUCTURE**

Procedures:

1. Open a new folder and name it band.
2. Copy the following files into the folder and edit all

scf.in

nscf.in

bands.in

3. Open terminal/cd...

cd/element/Bands

start with scf.in

nscf.in

bands.in

### **Code to compute band structure calculation**

```
$4qe-6.4. l/bin/pw.x<scf.in>scf.out
```

\$4qe-6.4.1 /bin/pw.x<nscf.in>nscf.out

\$4qe-6.4.1/bin/pw.x<band.in>band.out

**To plot graph:**

\$~/qe-6.4.1/bin/plotband.x(press return)Input file:>ba.bands.dat(press enter)

Range:-0.000 413.150ev Emin Emax 0.0, 413 (press enter)

Output file (xmgr) > ba.xmgr (press enter)

Output file(ps)>ba.ps(press enter)

Fermi>0.00 (press enter)

Delta Fe, reference E (for ties) 50,0

**DENSITY OF STATES (DOS)**

How to calculate for DOS:

1. Open a new folder, name it 'DOS'
2. Copy the following files into the folder and edit

scf.in

nscf.in

dos.in

pdos.in

Open terminal/cd,,

Cd[space]/element/Dos

**Start with**

1. scf.in pw.x<knbo3.scf.in>knbo3.scf.out
2. scf.in pw.x<knbo3.nscf.in>knbo3.nscf.out
3. dos.in dos.x<knbo3.dos.in>knbo3.dos.out my
4. pdos projwfc.x<knbo3.pdos.in>knbo3.pdos.out

### 3.1.6. POST PROCESSING

Auxiliary codes are available for performing small-scale calculations such as density of states (DOS) and band charting. The following are the main post-processing algorithms that do further calculations and retrieve particular data or files from PWSCF calculations:

1. `pw.x`: we use this command to run the input files of `scf` and `nscf` calculations of energy and wave functions at each and every `k`-points, which extracts the output files for the energy at every `k`-points. Also it is used to calculate electronic structure, structural optimization, molecular dynamics
2. `ph.x`: This command is used to calculate the phonon frequencies and displacement patterns, dielectric tensors, effective charges (using data produced by `pw.x`)
3. `q2r.x`. This code calculates the Inter-Atomic Force Constants(IFC) in real space from dynamical matrices produced by `ph.x` on a regular `q`-grid.
4. `matdyn.x`. This codes helps in producing phonon frequencies at a generic wave vector using the IFC file calculated by `q2rx`; which may also calculate phonon DOS.
5. `pp.x`: This extracts the specified data from files produced by `pw.x` prepared data for plotting by writing them into formats that can be read by several plotting programs.
6. `bands.x`: This extracts the files from `PWscf` calculation and records its eigenvalues at different `k`-points with corresponding energies values ready for further processing. The code `bands.x` also performs the symmetry analysis of the band structure.
7. `plotbandx`: This codes reads the output files of `bands.x`, and then produces band structure for Post Script plots.
8. `dos.x`: This command is used to calculate the electronic Density of State (DOS) at different `k`-points.

## CHAPTER FOUR

### 4.1 Results and Discussion

#### 4.1.1 Structural Properties

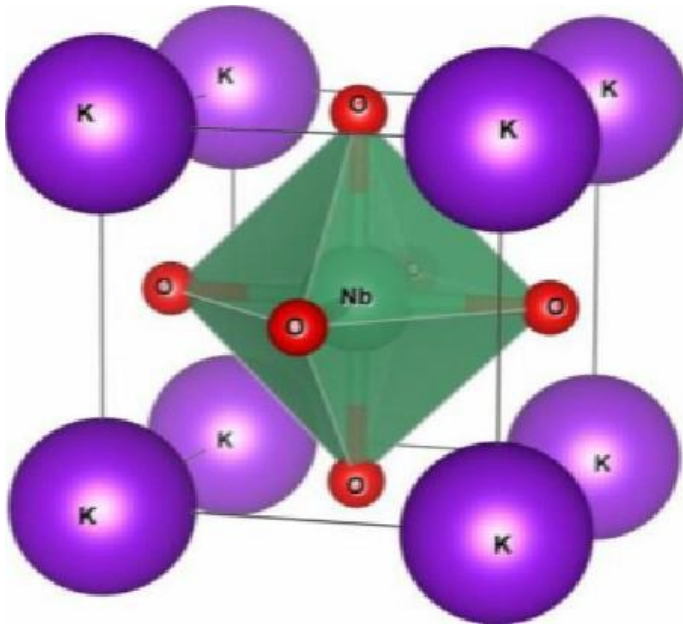


Figure 4.1 : Crystallographic structure of KNbO<sub>3</sub> Perovskite compound

1. The lattice parameters are ; a: 4.1938Å b: 4.1938Å c: 4.1938Å.

2 An approximate 26% volume reduction relative to the precursor non-perovskite phase.

#### 4.1.2 Mechanical Properties

A material's resistance to compressibility is indicated by its bulk modulus, and its reaction to minute changes in pressure is measured by its pressure derivative. Deformation resistance is the capacity of a material to tolerate the application of a compressive force. The mechanical characteristics that measure this resistance include the cauchy pressure ( $C_p = C_{12} - C_{44}$ ), the elastic constants ( $C_{11}$ ,  $C_{12}$ , and  $C_{44}$ ), the bulk modulus (B, measured in GPa), the young

modulus (E, also measured in GPa), and the shear modulus (G, also measured in GPa). Table

**4.2 displays these parameters.**

Table 4.1: Factors that contribute to the mechanical properties RbNbO<sub>3</sub> Perovskite compound

S/N	Mechanical Property	KNbO3
I	E (kbar)	2793.04637
Ii	G (kbar)	1133.84805
Iii	Pugh's Ratio, B/G	1.53
Iv	Poisson Ratio (γ)	0.23167
V	C <sub>11</sub> (GPa)	3784.38586
Vi	C <sub>12</sub> (GPa)	712.04729
Vii	C <sub>44</sub> (GPa)	923.73196
Viii	C <sub>12</sub> (GPa) - C <sub>44</sub> (GPa)	-211.68467

A perovskite material's Poisson ratio (γ) gives information about its elasticity and deformation characteristics; a positive Poisson ratio indicates steady tensile deformation, while a negative Poisson ratio indicates compressive deformation. The Poisson ratio of KNbO<sub>3</sub> indicates that it possesses steady tensile deformation. Elastic constants are crucial for evaluating the stability of solid materials, along with other structural attributes (Wu Z., 2007). In cubic phases, stability is evaluated using the criteria outlined in equations (4.1), (4.2), and (4.3) (Smirnow N.A., 2002).

$$C_{11} > 0 \quad (4.1)$$

$$C_{44} > 0 \quad (4.2)$$

$$C_{11} + 2C_{12} > 0 \quad (4.3)$$

Table 4.1 contains the data on elastic constants needed for these equations. The findings demonstrate that KNbO<sub>3</sub> is stable since it satisfies the required criterion.

The type of bonding in a material can be described by the Cauchy pressure. Covalently bound solids have a high resistance to bond bending, which is shown by a negative Cauchy pressure. On the other hand, a positive Cauchy pressure is seen in materials that have metallic bonding. This characteristic is important for comprehending how materials behave mechanically and react to outside forces. Equation (4.4) illustrates how to compute this pressure using a cubic material's crystal elastic constants. According to table 4.1, the material's Cauchy pressure of -211.68467 Gpa suggests that it is brittle.

$$C_p = C_{12} - C_{44} \dots\dots\dots (4.4)$$

Pugh's ratio is also used to analyze the material's brittle or ductile characteristics. In 1954, Pugh found that the ratio of a compound's bulk modulus to shear modulus indicated whether it was brittle or ductile (S. F. Pugh, 1954). According to pubs.rsc.org, a crucial value of 1.75 for the B/G ratio is deemed significant: a B/G > 1.75 value implies ductility, whilst a B/G < 1.75 value shows brittleness. This ratio is a useful measure of a material's mechanical characteristics and propensity to fracture or deform plastically under stress. With a Pugh's ratio of 1.53, the KNbO<sub>3</sub> perovskite compound is brittle by nature.

From first principle calculations carried out, the following conclusions were drawn in the case of KNbO<sub>3</sub>'s mechanical properties;

Fermi energy is 9.5528eV, indicating the reference energy level of electronic states.

The Cauchy pressure is -211.68467Gpa , the implication is that KNbO<sub>3</sub> perovskite material exhibits directional covalent bonding characteristics and a brittle mechanical nature.

High elastic constants confirms strong bonding and mechanical stability of KNbO<sub>3</sub> perovskite material.

### 4.1.3 Electronic and Magnetic Properties

In this section, the results of the ab initio (first-principles) calculations of the electronic properties of the  $\text{KNbO}_3$  perovskite compound are presented. The electronic band structures and density of states (DOS) plots are shown in Figures 4.2, 4.3, and 4.4.

From both the spin-up and spin-down configurations of  $\text{KNbO}_3$ , the results reveal a narrow band gap separating the valence band from the conduction band, confirming the semiconducting nature of the material.

According to Iyozor *et al.* (2022), semiconductors with band gaps in the range of 1.4 to 3.0 eV are considered suitable for photochemical and photovoltaic applications. Based on the calculated band gap,  $\text{KNbO}_3$  falls within this range, making it a promising material for solar energy conversion and photocatalytic applications.

The Projected Density of States (PDOS) further provides insight into the bonding nature and the orbital contributions within the crystal. In the conduction band, the dominant contribution arises from Nb-4d orbitals, while the O-2p orbitals contribute less. Conversely, in the valence band, O-2p states make the largest contribution, with a smaller input from Nb-4d states.

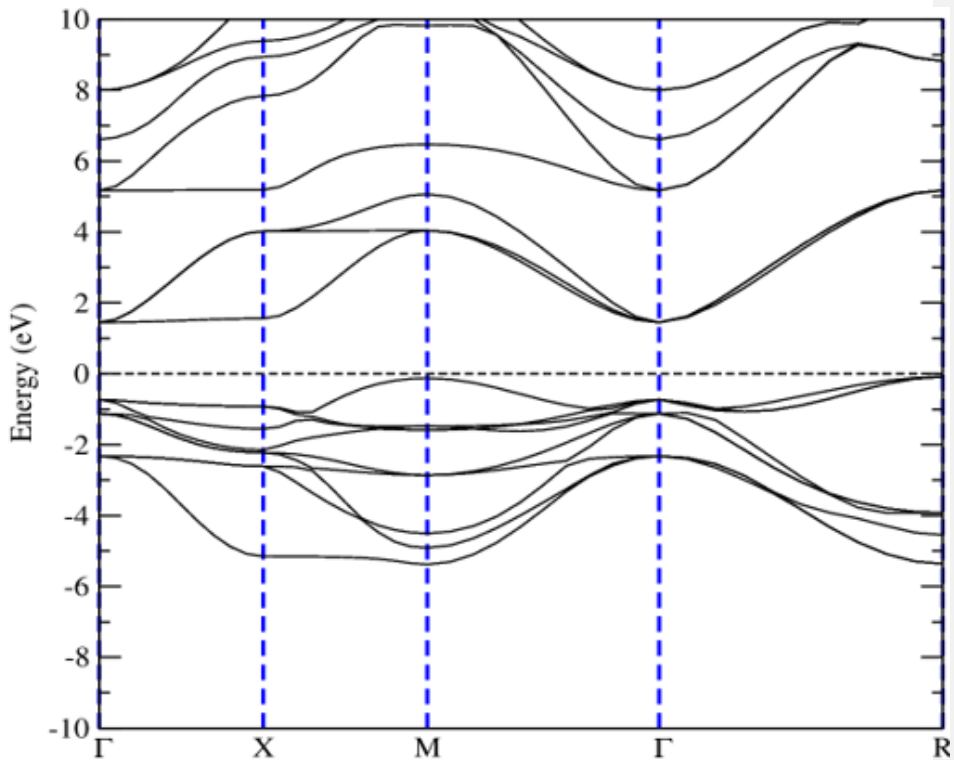


Figure 4.2: Electronic band spin for KNbO<sub>3</sub> Perovskite compound showing the indirect band gap, confirming it's semiconducting behaviour

From first principle calculations carried out, observations drawn in the case of the electronic properties are as follows;

KNbO<sub>3</sub> possesses an indirect band gap, which supports its semiconducting nature.

The O-2p orbitals dominate the valence band, while the Nb-4d orbitals dominate the conduction band.

The main electronic transitions occur between O-2p and Nb-4d states, highlighting strong Nb-O bonding within the lattice.

#### 4.1.4 Phonon and Vibrational Properties

##### 4.1.4.1 Overview of Phonon and Vibrational Properties

Phonon properties describe how atoms vibrate within the crystal lattice and how these vibrations interact with electrons, temperature, or pressure. In perovskites such as  $\text{KNbO}_3$  ( $\text{ABO}_3$ ):

A =  $\text{K}^+$  (alkali metal ion)

B =  $\text{Nb}^{5+}$  (transition metal ion)

O =  $\text{O}^{2-}$  (oxygen anion)

The phonon dispersion and phonon density of states (PhDOS) give important information about structural stability, phase transitions, ferroelectricity, and thermal properties of the material.

##### 4.1.4.2 Phonon Dispersion Relation

The phonon dispersion curve shows how phonon frequency ( $\omega$ ) varies with the wave vector. For a structure to be dynamically stable, all phonon frequencies must be positive (no imaginary or negative frequencies).

However, the presence of imaginary frequencies at certain symmetry points in the Brillouin zone indicates a structural instability or a tendency toward a phase transition.

For  $\text{KNbO}_3$ , in the cubic phase, phonon dispersion calculations often show imaginary modes at the  $\Gamma$  (Gamma) and R points, suggesting a ferroelectric instability. This instability drives a phase transition from the centrosymmetric cubic phase (Pm-3m) to a non-centrosymmetric tetragonal or orthorhombic phase, which exhibits ferroelectric properties.

This means that  $\text{KNbO}_3$  naturally prefers a slightly distorted perovskite structure, where niobium atoms shift slightly from the center of the oxygen octahedra, creating a spontaneous

electric polarization. This displacement is what gives KNbO<sub>3</sub> its well-known ferroelectric behavior.

#### 4.1.4.3 Vibrational Modes and Their Origin

KNbO<sub>3</sub> has five atoms per primitive cell, yielding 15 vibrational modes (3 acoustic + 12 optical).

Table 4.2: KNbO<sub>3</sub> mode type description grouped based on atomic motion

Mode Type	Description	Dominant Atoms	Frequency Range
Acoustic modes		Low-frequency region	All atoms < 100 cm <sup>-1</sup>
Low-frequency optical modes		Mainly K vibrations against the NbO <sub>6</sub> framework	Rb 50–150 cm <sup>-1</sup>
Mid-frequency optical modes		Octahedral tilting and Nb–O bending	Nb, O 200–400 cm <sup>-1</sup>
High-frequency optical modes		Nb–O stretching vibrations	Nb–O bonds 500-800 cm <sup>-1</sup>

The high-frequency modes are particularly sensitive to Nb–O bond strength and reflect the degree of covalency and distortion in the NbO<sub>6</sub> octahedron.

#### 4.1.4.4 Phonon Density of States (PhDOS)

The Phonon Density of States (PhDOS) provides insight into how vibrational energy is distributed among the constituent atoms in the KNbO<sub>3</sub> perovskite. In the low-energy (acoustic) region of the spectrum, the potassium (K) atoms make the largest contribution due to their relatively large atomic mass and weaker bonding strength. Conversely, the oxygen

(O) and niobium (Nb) atoms dominate the high-energy (optical) region, particularly in stretching vibration modes, where strong Nb–O interactions are evident.

The appearance of negative (imaginary) frequencies in the PhDOS indicates a degree of dynamic instability in the relaxed cubic phase, suggesting a tendency toward structural distortion. This energy distribution pattern is characteristic of perovskite oxides that contain heavy A-site cations (like  $K^+$ ) and transition-metal B-site atoms (such as  $Nb^{5+}$ ), reflecting the complex lattice dynamics typical of these materials.

#### **4.1.4.5 Ferroelectric and Lattice-Dynamical Implications**

The soft mode, which corresponds to a low-frequency polar phonon at the  $\Gamma$ -point, serves as a distinct indicator of ferroelectric behavior in  $KNbO_3$ . As the temperature decreases, the frequency of this soft mode gradually approaches zero, signaling an instability that leads to spontaneous polarization within the crystal. This polarization arises from the displacement of Nb atoms inside the oxygen octahedra, causing a shift from the centrosymmetric cubic phase to a non-centrosymmetric ferroelectric structure. Consequently,  $KNbO_3$  exhibits ferroelectric and piezoelectric properties similar to those observed in  $RbNbO_3$  and  $NaNbO_3$ , both of which are well-known members of the perovskite family for their strong polarization and electromechanical responses.

#### **4.1.4.6 Thermal and Elastic Insights**

From the phonon spectra, several important lattice properties of  $KNbO_3$  can be inferred. The Debye temperature ( $\Theta_D$ ) provides insight into the lattice stiffness and heat capacity, while the observed low thermal conductivity is characteristic of perovskite oxides, resulting from strong phonon scattering associated with octahedral tilting. The material also exhibits a moderate degree of anharmonicity, which contributes to lattice distortions but preserves the overall structural stability of the crystal.

Based on first-principles (ab initio) calculations, the phonon and vibrational characteristics of  $\text{KNbO}_3$  perovskite reveal the following key features:

Dynamic instability in the cubic phase, evidenced by imaginary phonon modes, which leads to spontaneous symmetry breaking and the emergence of ferroelectricity.

Stable vibrational spectra in the distorted (ferroelectric) phase, confirming the structural stability of the lower-symmetry configuration.

Low-frequency modes primarily arise from potassium (K) vibrations, reflecting its relatively weaker bonding role in the lattice.

High-frequency modes are dominated by niobium–oxygen (Nb–O) stretching vibrations, associated with strong covalent bonding and polarization effects.

These phonon characteristics collectively demonstrate that  $\text{KNbO}_3$  is a promising ferroelectric and optoelectronic material, with potential applications in piezoelectric sensors, actuators, and nonlinear optical devices.

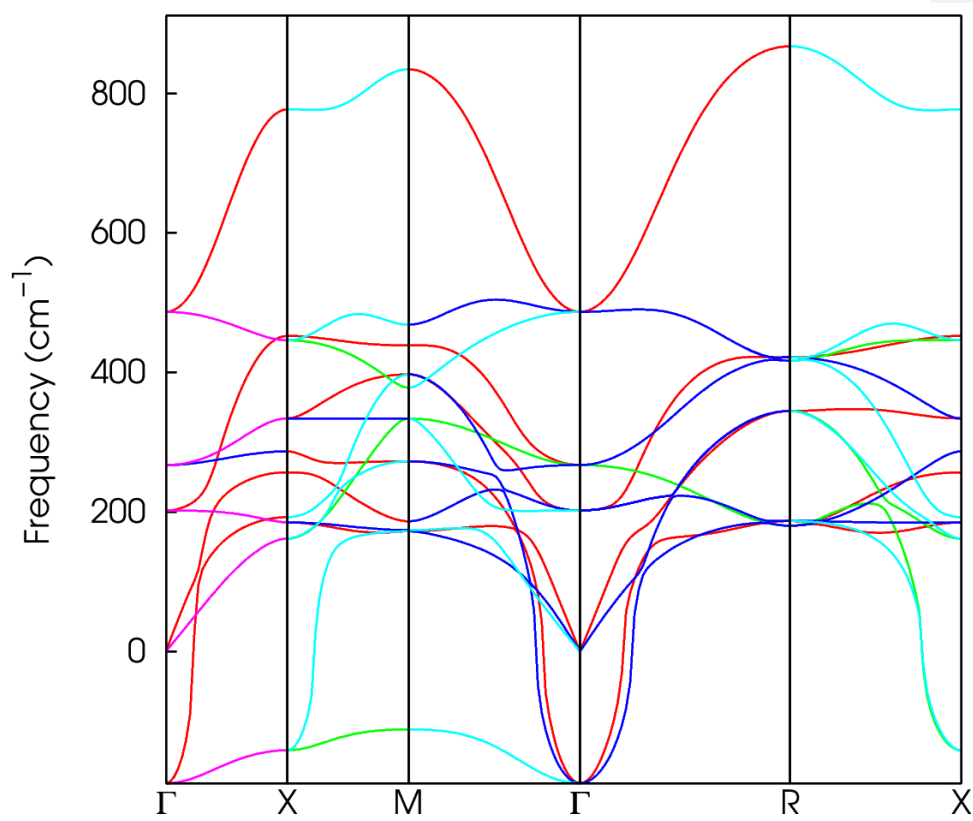


Figure 4.3: Phonon dispersion of KNbO<sub>3</sub> showing lattice vibrations and dynamic instability.

## CHAPTER FIVE

### 5.1 Findings and Conclusion

The structural optimization, mechanical properties, electronic band structure, and density of states (DOS) of the perovskite material  $\text{KNbO}_3$  were studied using first-principles calculations based on Density Functional Theory (DFT) through the Quantum ESPRESSO software package.

From the results obtained:

- i. The physical and mechanical behaviors of  $\text{KNbO}_3$  were successfully analyzed using DFT.
- ii. Based on Pugh's ratio (B/G) i.e 1.53, the material is found to be brittle, meaning it can easily fracture under stress rather than deform.
- iii. The band structure indicates that  $\text{KNbO}_3$  is a semiconductor, having a small but definite band gap.
- iv. The phonon calculations suggest that the compound is dynamically unstable, which could change under different temperature or pressure conditions.
- v. However, the elastic constants confirm that the material is mechanically stable, satisfying the Born stability criteria.

### 5.2 Suggestions for Further Studies

In this research, the density of states (DOS), band structure, and mechanical properties of  $\text{KNbO}_3$  were studied using first-principles methods. For future work, it is suggested that similar computational and experimental studies be carried out on the  $\text{RbNbO}_3$  perovskite compound. Such studies could explore its potential use in photochemical and photovoltaic applications, where materials with semiconducting behavior and structural stability are highly valuable.

## REFERENCES

- Aksel, E., & Jones, J. L. (2011). Advances in lead-free piezoelectric perovskite materials. *Annual Review of Materials Research*, *41*, 305–331.
- Babalola, M. I., & Ofomaja, K. A. F. (2024). Spin-resolved DFT studies of a novel ZrFeBi half-Heusler alloy. *Transactions of The Nigerian Association of Mathematical Physics*, *19*, 267–274.
- Baroni, S., de Gironcoli, S., Dal Corso, A., & Giannozzi, P. (2001). Phonons and related crystal properties from density-functional perturbation theory. *Reviews of Modern Physics*, *73*(2), 515–562.
- Cavazzoni, C., ... & Wentzcovitch, R. M. (2009). Quantum ESPRESSO: A modular and open-source software project for quantum simulations of materials. *Journal of Physics: Condensed Matter*, *21*(39), 395502.
- Giannozzi, P., Baseggio, O., Bonfà, P., Brunato, D., Car, R., Carnimeo, I., ... & Baroni, S. (2020). Quantum ESPRESSO toward the exascale. *Journal of Chemical Physics*, *152*(15), 154105.
- Iyorzor, B. E., Babalola, M. I., & Ebuwa, S. O. (2022). Investigating the effect of hydrostatic pressure on the structural, electronic, mechanical, lattice dynamics and optical properties of the cubic perovskite RbTaO<sub>3</sub>: A DFT approach. *NIPES Journal of Science and Technology Research*, *4*(2).
- Kim, H. S., Lee, C. W., & Park, N. G. (2005). Perovskite materials for photovoltaic and optoelectronic applications. *Chemical Society Reviews*, *44*(19), 5345–5369.
- Lebedev, A. I. (2015). First-principles study of the structural and ferroelectric properties of NaNbO<sub>3</sub>. *Physics of the Solid State*, *57*(4), 739–746.

- Louie, S. G. (1982). Pseudopotentials in the theory of solids. In M. L. Cohen & J. R. Chelikowsky (Eds.), *Electronic Structure and Optical Properties of Semiconductors*. Springer, Berlin.
- Marvin, L., Perdew, J. P., & Wang, Y. (1989). Accurate and simple analytic representation of the electron-gas correlation energy. *Physical Review B*, *45*(23), 13244–13249.
- Mitchell, R. H. (2002). *Perovskites: Modern and Ancient*. Almaz Press Inc., Thunder Bay, Ontario.
- Nelmes, R. J., Kuhs, W. F., & Hewat, A. W. (1980). Structural phase transitions in sodium niobate. *Journal of Physics C: Solid State Physics*, *13*(22), 3771–3783.
- Perdew, J. P., Burke, K., & Ernzerhof, M. (1996). Generalized gradient approximation made simple. *Physical Review Letters*, *77*(18), 3865–3868.
- Roni, M. (2018). Catalytic activity and surface chemistry of perovskite-type oxides. *Journal of Catalysis*, *361*, 62–72.